Lecture 14:
Current Topics I
## And
Unexpected Physics!

D. H. Dowell, SLAC

- *The objective of this lecture is to describe some of the near term challenges of injectors for 4th generation light sources. Measurements of an unexpected microbunching instability will be presented. Cathode limitations and a means for improving it is presented.*

- *The student will learn about how coherent synchrotron radiation degrades the electron beam quality and confuses the diagnostics and how this is mitigated with the laser heater. And will learn about "structured" cathodes.*

Coherent Synchrotron Radiation Induced Emittance Growth

Electron Microbunch Traveling in an Arc
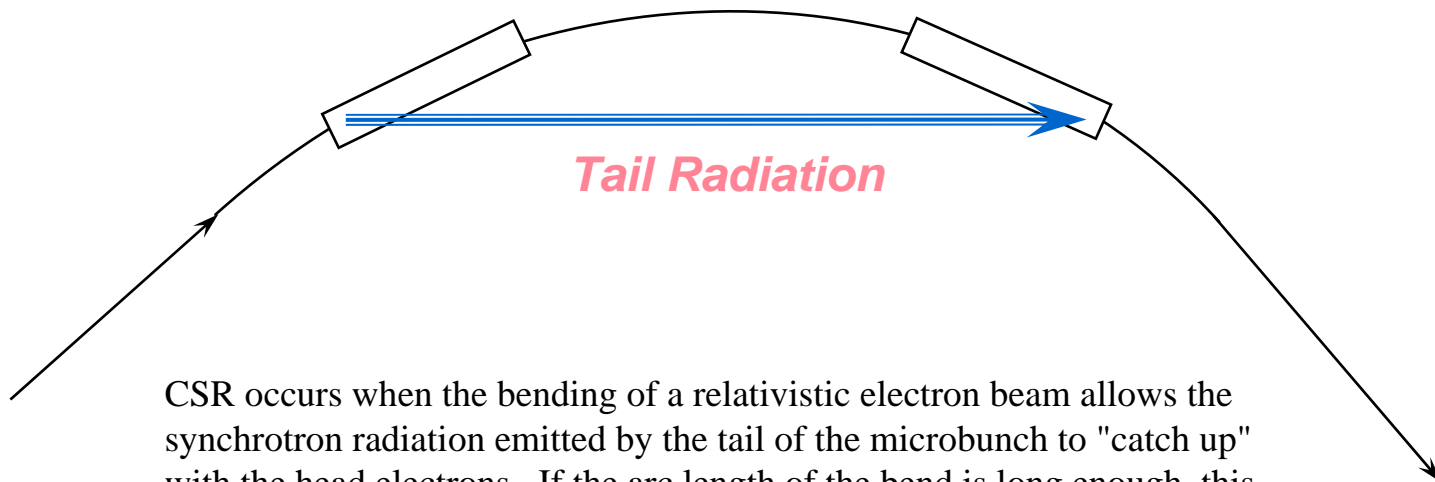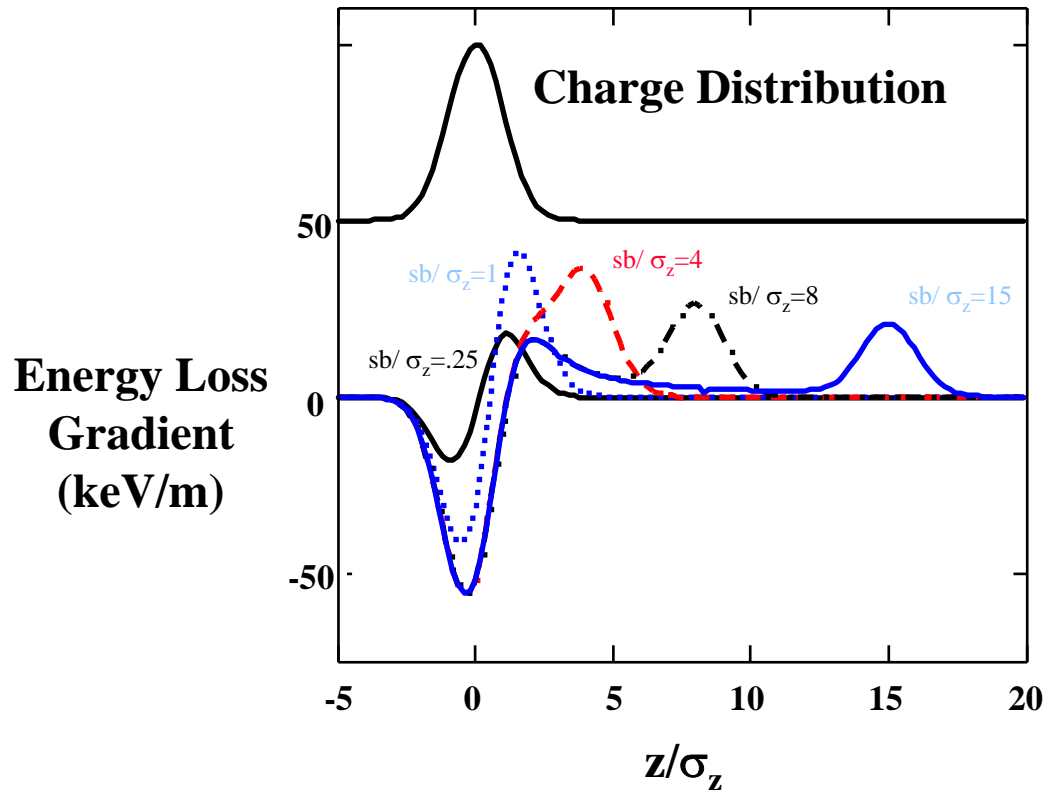
Tail Radiation

CSR occurs when the bending of a relativistic electron beam allows the synchrotron radiation emitted by the tail of the microbunch to "catch up" with the head electrons. If the arc length of the bend is long enough, this radiation sweeps along the entire length of the microbunch and transfers energy from the tail to the head. Therefore CSR tends to increase the energy of the head while lowering that of the tail.

Ref: Y.S. Derbenev et al., DESY TESLA-FEL Technical Note 95-05(1995)

# *Transient CSR Radiation at the Magnetic Field Boundary*

Charge Distribution

$$\lambda \, (\mathbf{s}) = \frac{1}{\sqrt{2\pi} \, \sigma_{\mathbf{z}}} e^{-\mathbf{s}^2/2\sigma_{\mathbf{z}}^2}$$

Energy Loss Gradient (keV/m)

50

sb/σ_z=1   sb/σ_z=4   sb/σ_z=8   sb/σ_z=15

sb/σ_z=.25

0

-50

-5   0   5   10   15   20

$$\mathbf{z}/\sigma_{\mathbf{z}}$$

$$\mathbf{F_1(sb, x)} = \int\limits_{\mathbf{x-sb}}^{\mathbf{x}} \frac{\mathbf{dx'}}{\mathbf{(x-x')}^{1/3}} \frac{\partial \, \lambda(\mathbf{x'})}{\partial \, \mathbf{x'}}$$

Ref: D.H. Dowell and P.G. O'Shea, "Coherent Synchrotron Radiation Induced Emittance Growth in a Chicane Buncher", contribution to PAC'97.
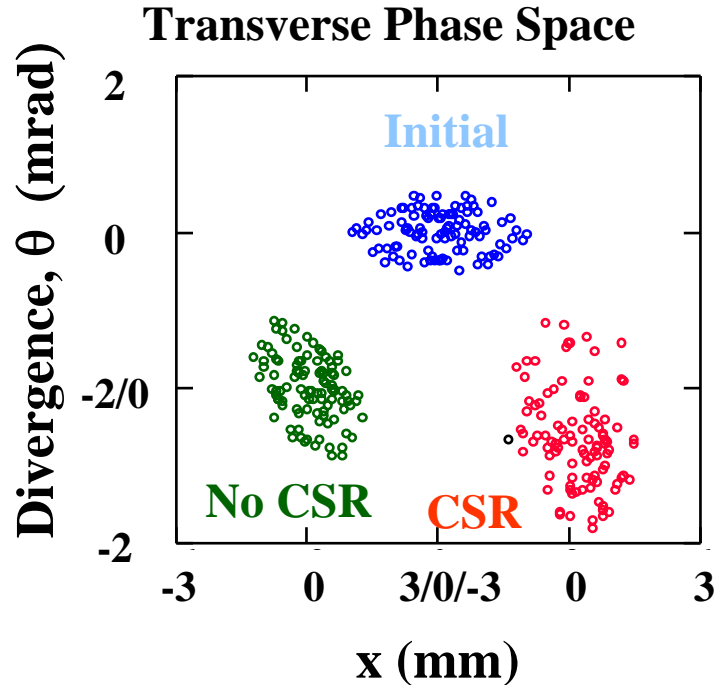
Boeing Chicane Buncher

-19.5°   **-19.5°**

30°   **30°**

384 mm   **60°**   **384 mm**
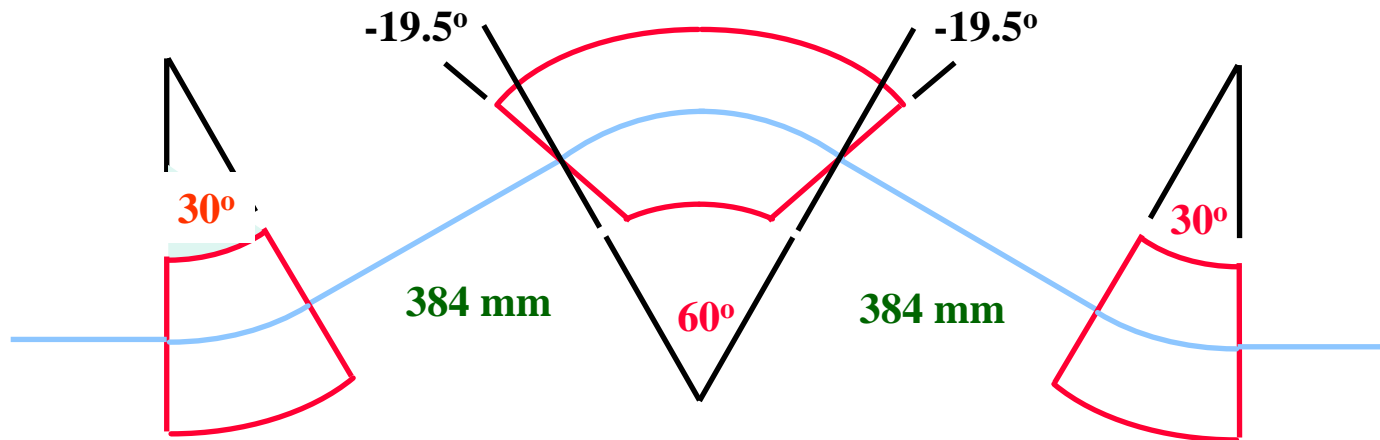
Achromatic chicane composed of three n=1/2 dipoles.

Coherent Synchrotron Radiation Induced Emittance Growth

**Transverse Phase Space**

θ−z Correlation

The initial and final transverse phase space distributions, with and without CSR, when the microbunch is compressed. The distributions are offset for display only.
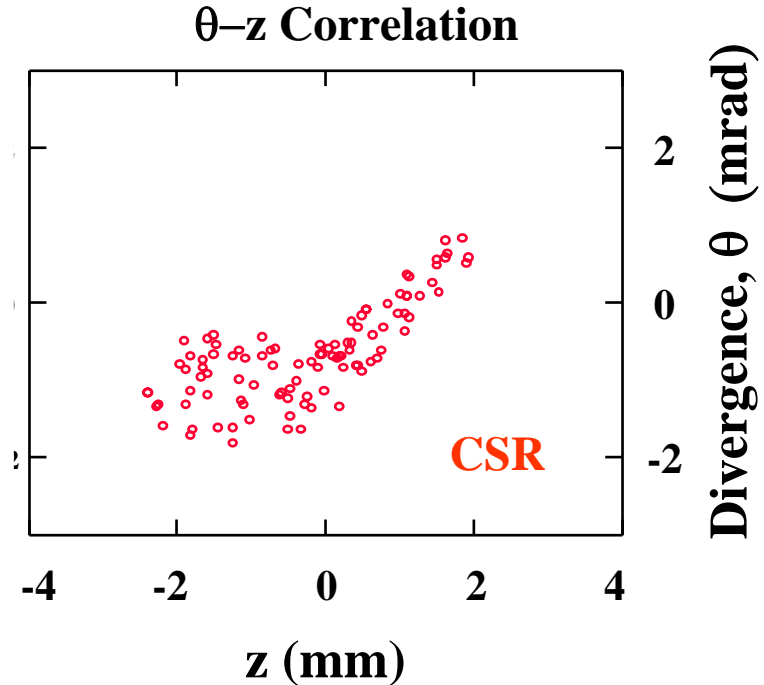
The correlation of divergence with longitudinal position at the exit of the chicane due to CSR.

Comparison of experiment with PARMELA and CSR emittance growth calculations.
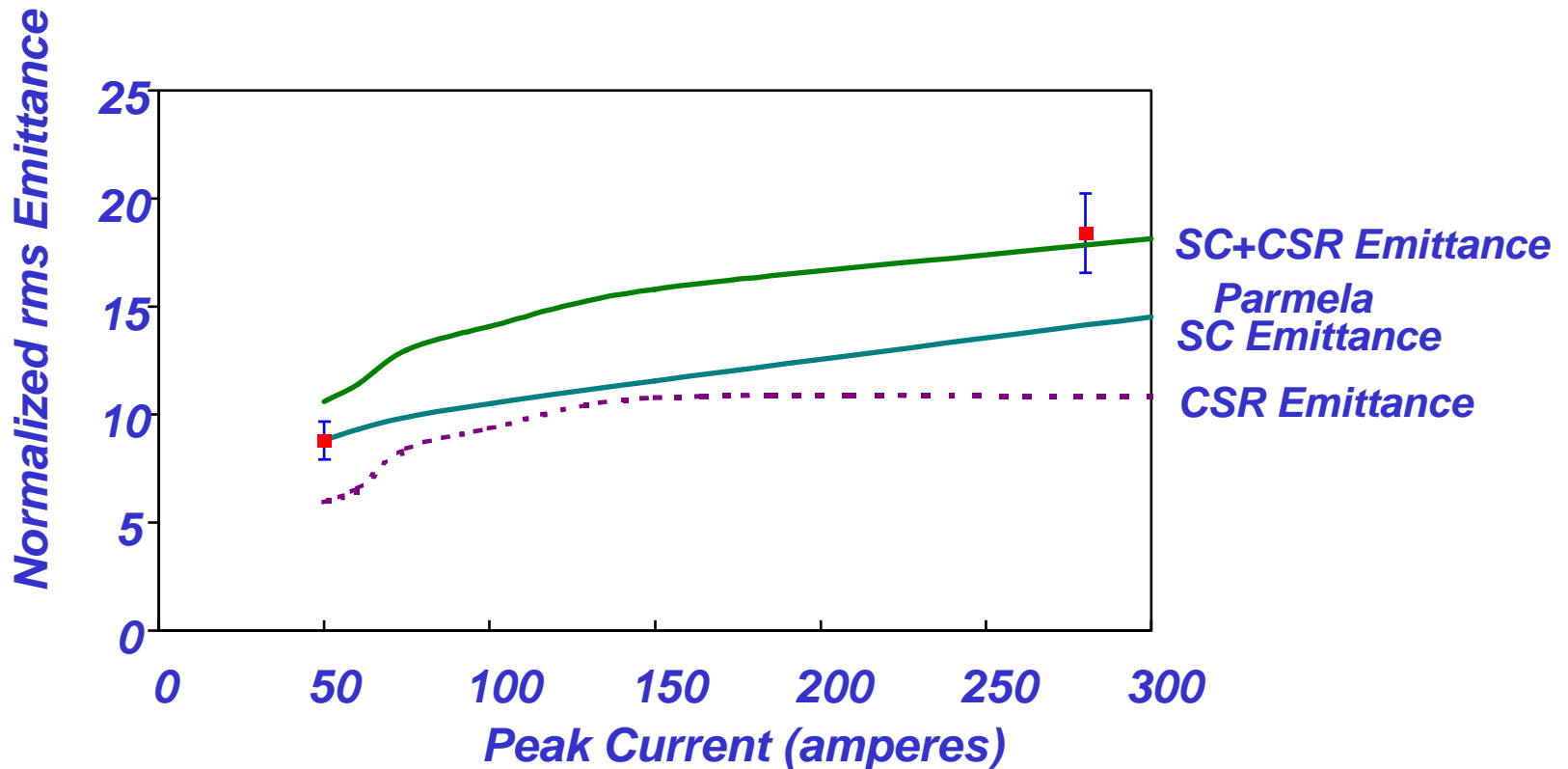
Suppression of microbunching instability in the linac coherent light source

Z. Huang,[1,*] M. Borland,[2] P. Emma,[1] J. Wu,[1] C. Limborg,[1] G. Stupakov,[1] and J. Welch[1]

[1]Stanford Linear Accelerator Center, Stanford, California 94309, USA
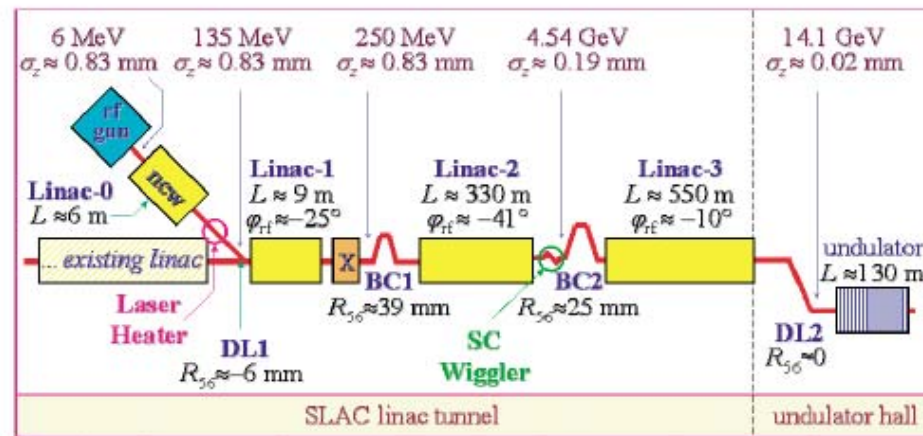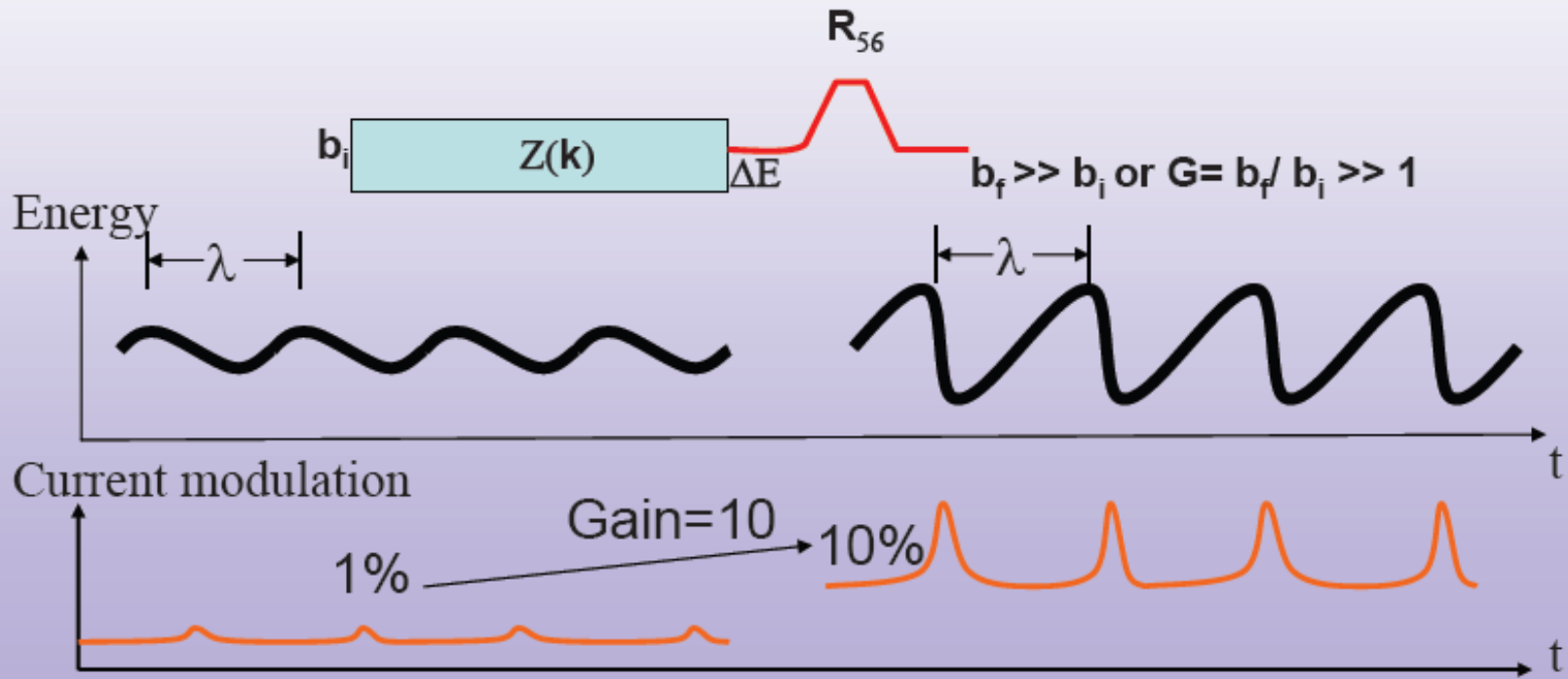[2]Argonne National Laboratory, Argonne, Illinois 60439, USA

FIG. 1. (Color) Layout of the LCLS accelerator system with two Landau damping options: a superconducting (SC) wiggler at 4.5 GeV or a laser heater at 135 MeV.

Microbunching instability first observed in simulations by M. Borland (ANL).

Microbunching instability

- Initial density modulation induces energy modulation through long. impedance Z(k), converted to more density modulation by a chicane → growth of local energy spread/emittance!

R_{56}

b_i $\quad$ Z(k) $\quad$ ΔE $\quad$ $b_f \gg b_i$ or $G = b_f / b_i \gg 1$

Energy

λ $\qquad$ λ

t

Current modulation

1% $\xrightarrow{\text{Gain=10}}$ 10%

t

LCLS Laser Heater Review
March 1, 2004

4

Zhirong Huang, SLAC
zrh@slac.stanford.edu

Stanford
Linear
Accelerator
Center

High Brightness Electron Injectors for
Light Sources - January 14-18 2007

Lecture 14
D.H. Dowell, S. Lidia, J.F. Schmerge

SDL RF zero-phasing measurement

- RF zero-phasing method can be used to extract LSC-induced energy modulation in the linac (Shaftan/Huang)
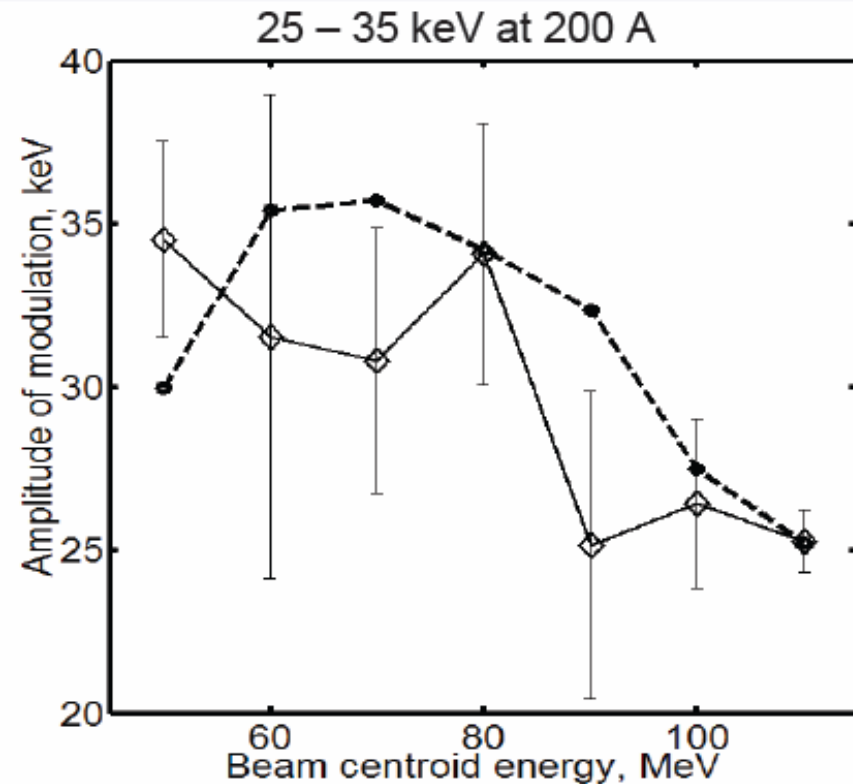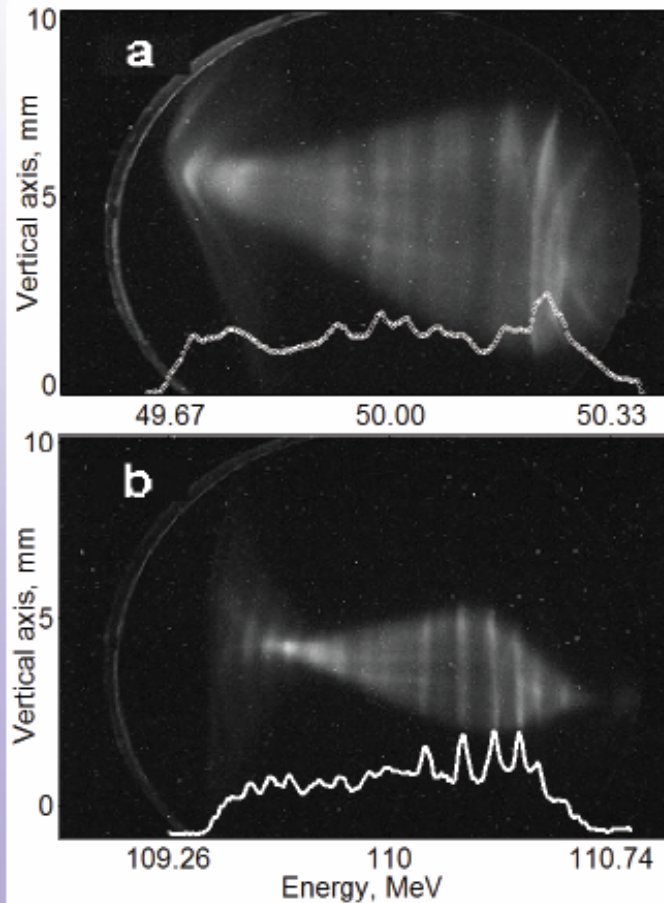
Zhirong Huang, SLAC
zrh@slac.stanford.edu

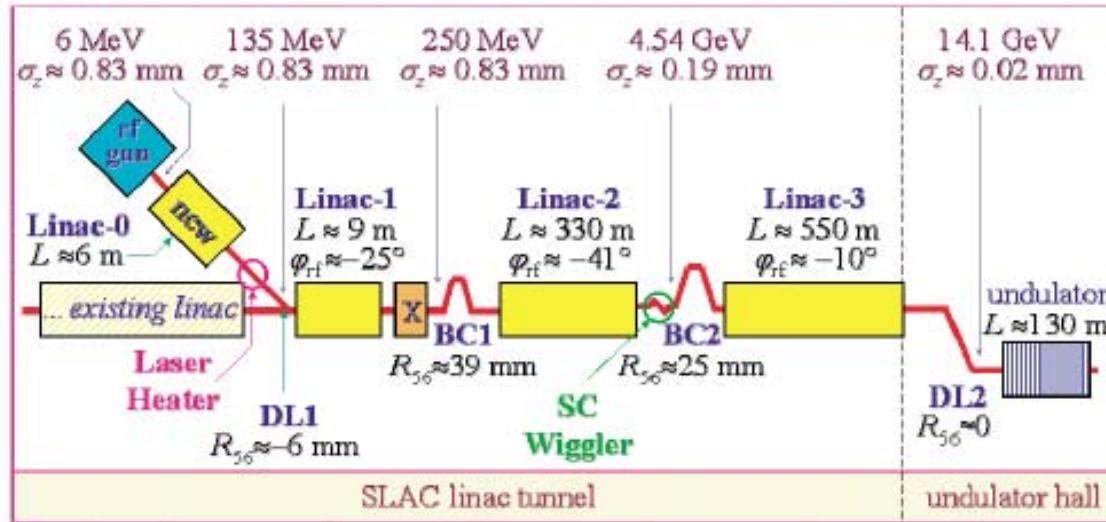# Possible Schemes for Damping the CSR Instability

FIG. 1. (Color) Layout of the LCLS accelerator system with two Landau damping options: a superconducting (SC) wiggler at 4.5 GeV or a laser heater at 135 MeV.
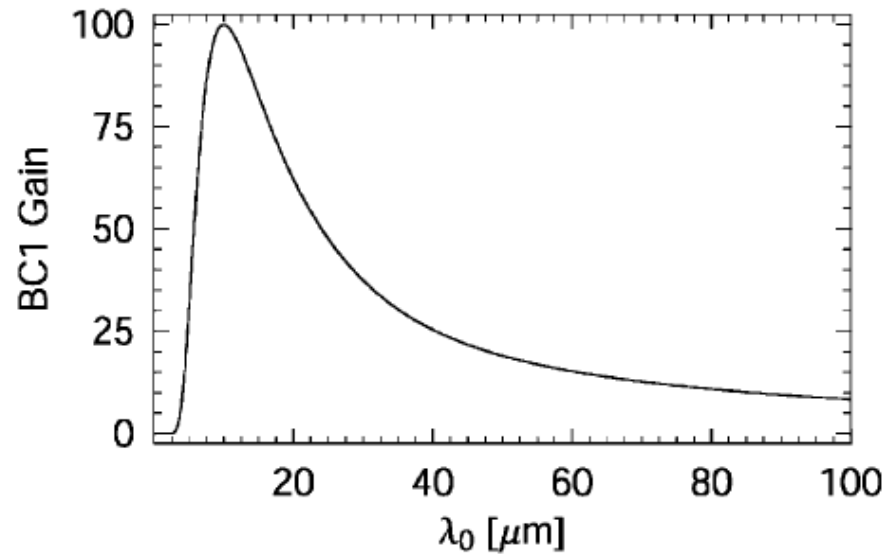
Microbunching Gain after BC1

FIG. 3. Microbunching gain after BC1 as a function of the initial modulation wavelength λ_0.

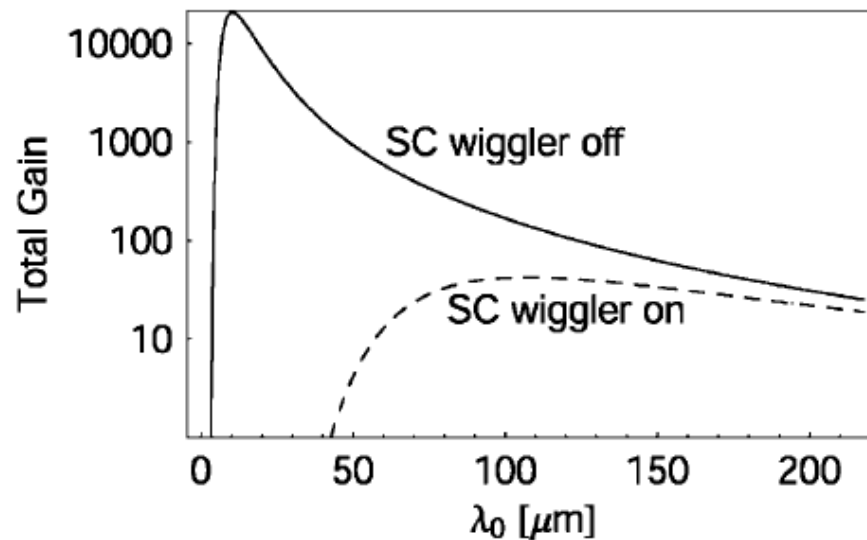# *Suppression of Microbunching Instability with a Super Conducting Undulator*

FIG. 5. Microbunching gain after BC2 as a function of the initial modulation wavelength λ_0 with the SC wiggler off (solid curve) and on (dashed curve).

To be efficient, the undulator has to be at high energy, 4.5 GeV, when damage is already done.
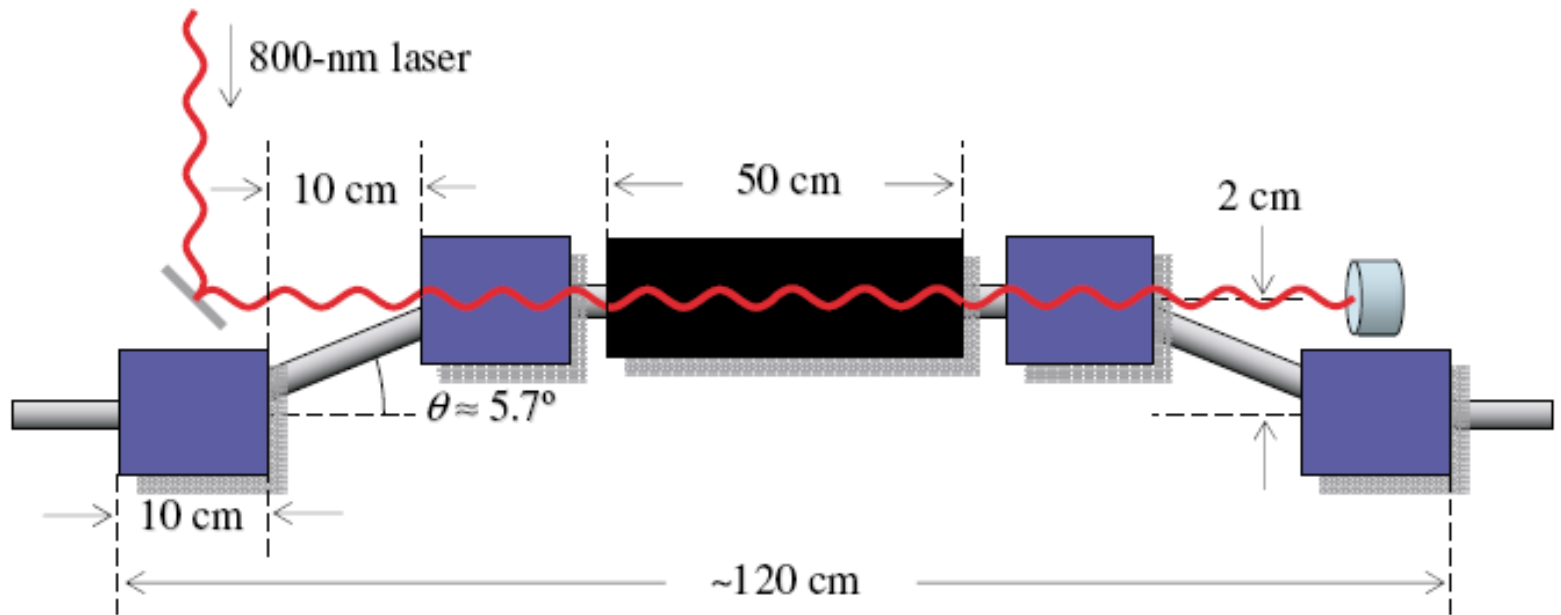
Laser Heater

FIG. 14. (Color) Layout of the LCLS laser heater inside a magnetic chicane at 135 MeV.
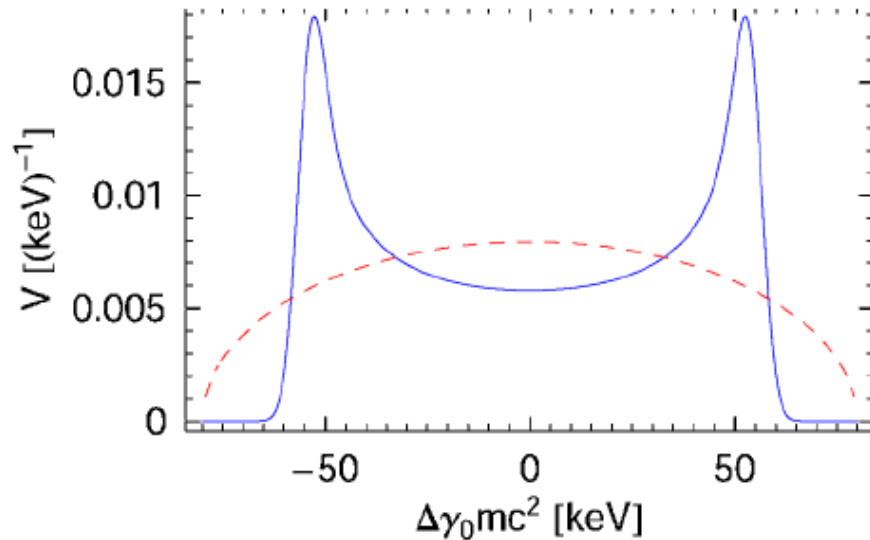
Energy Distribution After Laser Heater

FIG. 8. (Color) Electron energy distribution after the laser heater for a large laser spot (blue solid curve) and for a matched laser spot (red dashed curve). The laser powers are given in Table II so that the rms energy spread $\sigma_{\gamma_L} mc^2 \approx 40$ keV for both distributions.
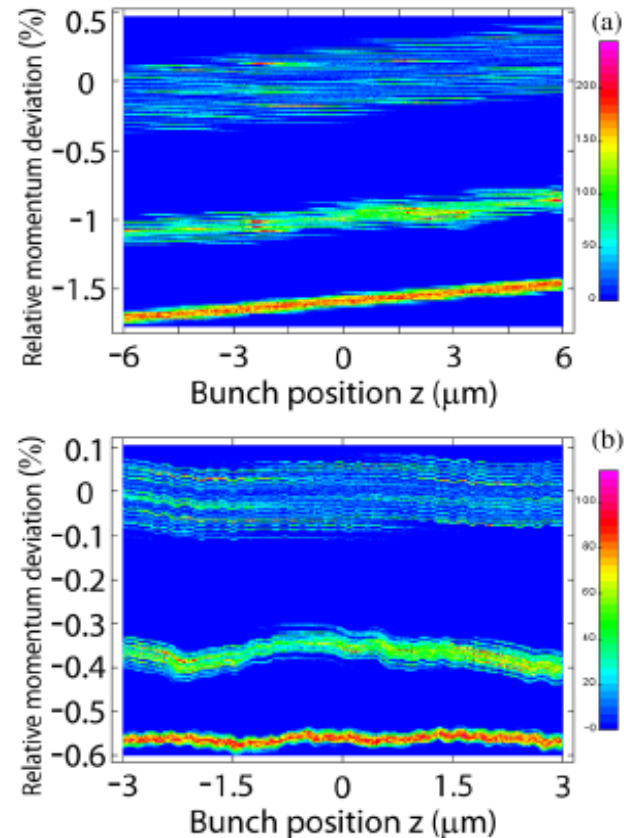

FIG. 12. (Color) Central portion of the longitudinal phase space without a laser heater (upper), in the presence of a laser heater with $\sigma_r = 1.5$ mm (middle) and with $\sigma_r = 175$ μm (lower). Curves offset vertically for clarity. Simulations are seeded with 1% initial density modulation at $\lambda_0 = 30$ μm. (a) End of BC2 at 4.5 GeV. (b) Undulator entrance at 14 GeV.
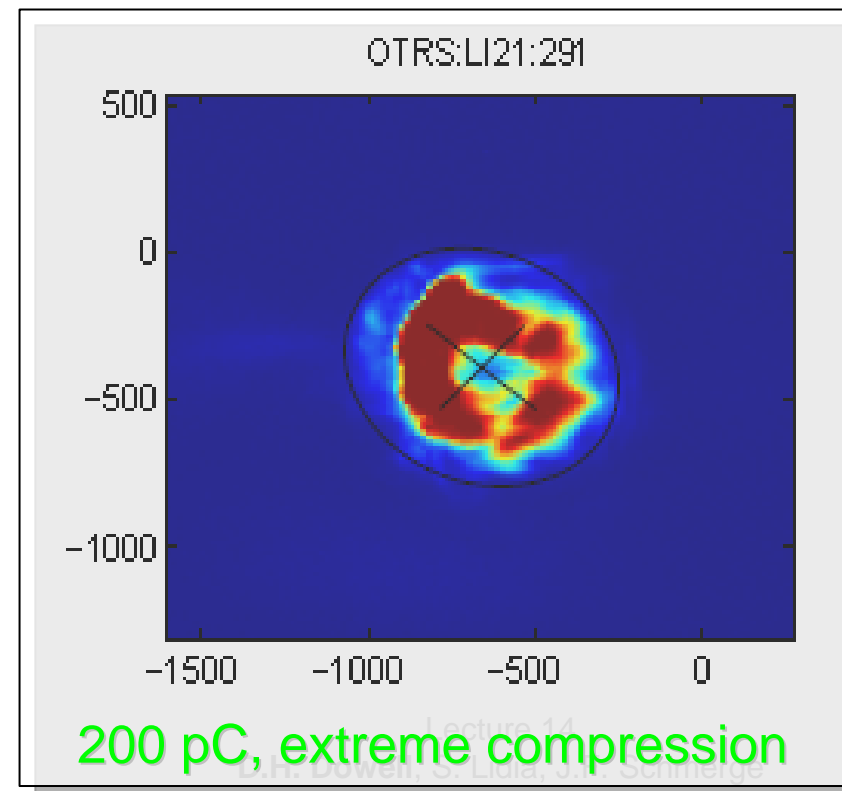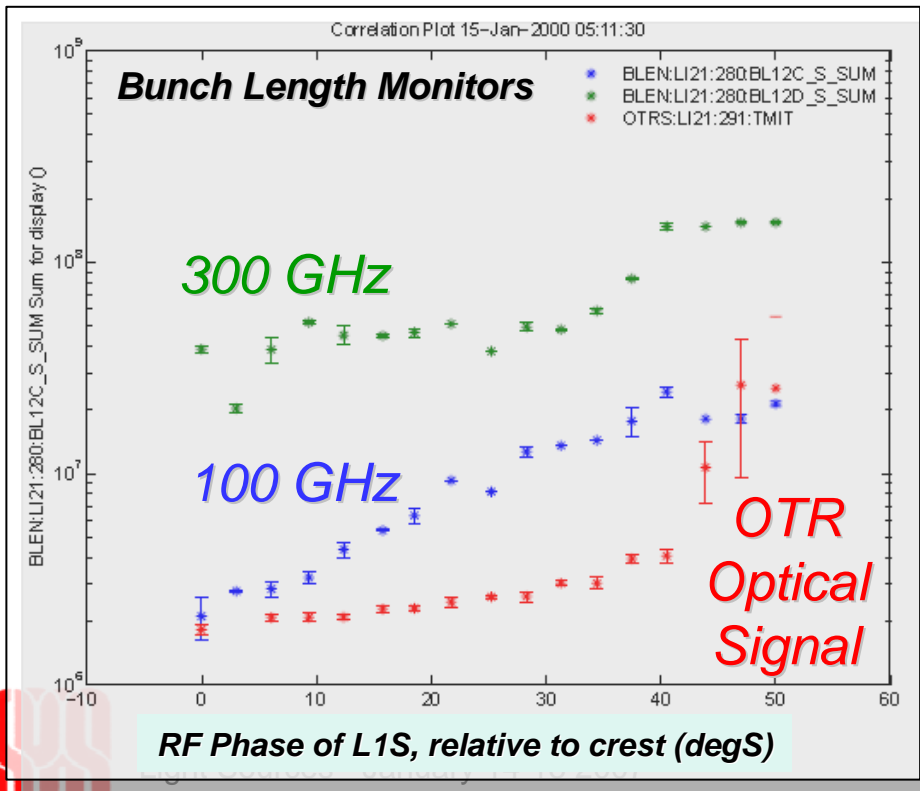
Unexpected Physics! **Coherent OTR with Maximum Compression**

Generation of COTR in the Visible Spectrum Indicates Spike & Interferes with Using OTR for Emittance Measurements.
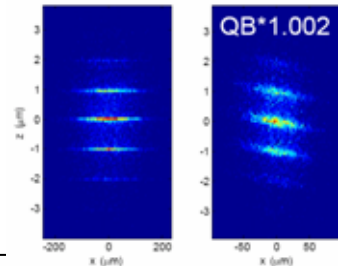
OTR Light increases by 10-100 with maximum compression

OTR Images Can Produce "Ring-Like" Shapes!

Correlation Plot 15-Jan-2000 05:11:30

Bunch Length Monitors

- BLEN:LI21:280:BL12C_S_SUM
- BLEN:LI21:280:BL12D_S_SUM
- OTRS:LI21:291:TMIT

BLEN:LI21:280:BL12C_S_SUM Sum for display 0

300 GHz

100 GHz

OTR Optical Signal

RF Phase of L1S, relative to crest (degS)

OTRS:LI21:291
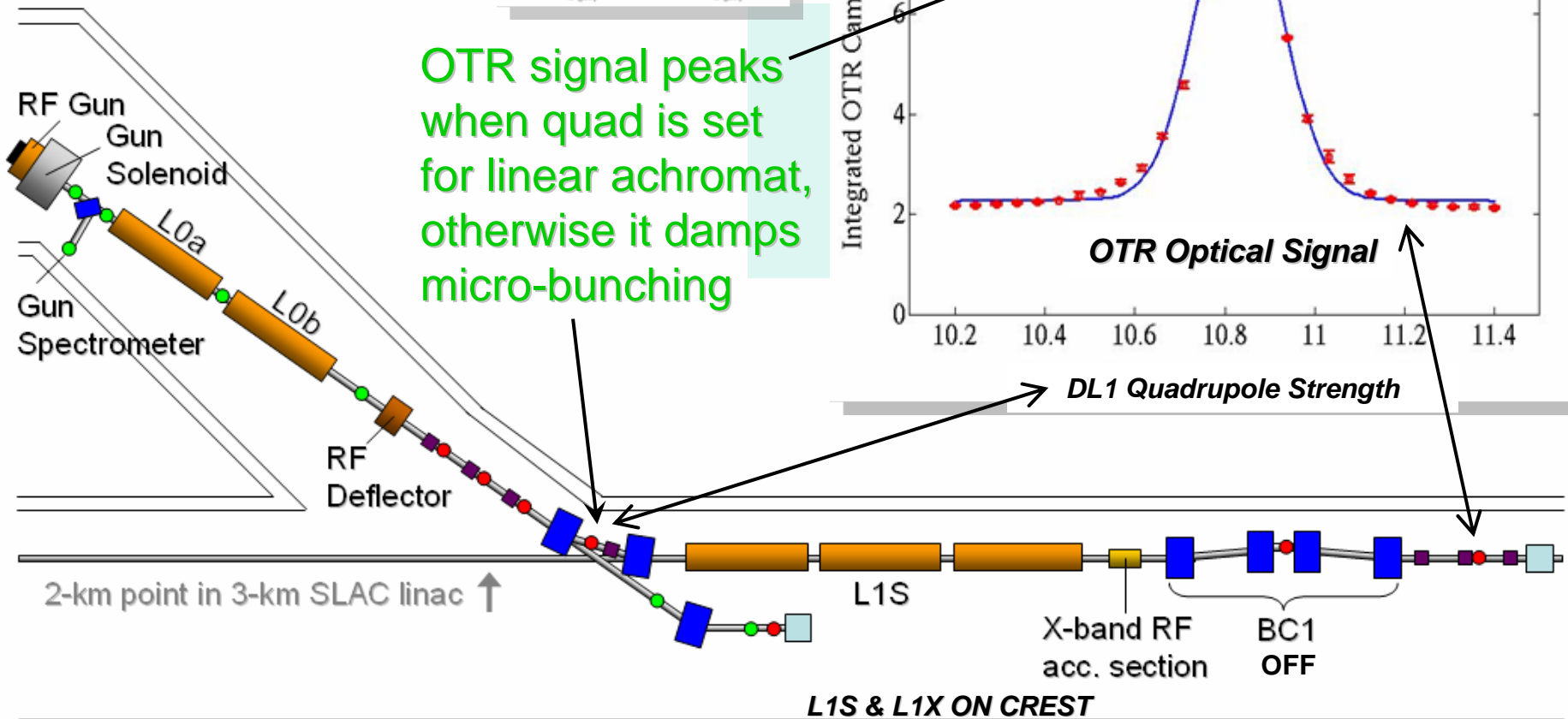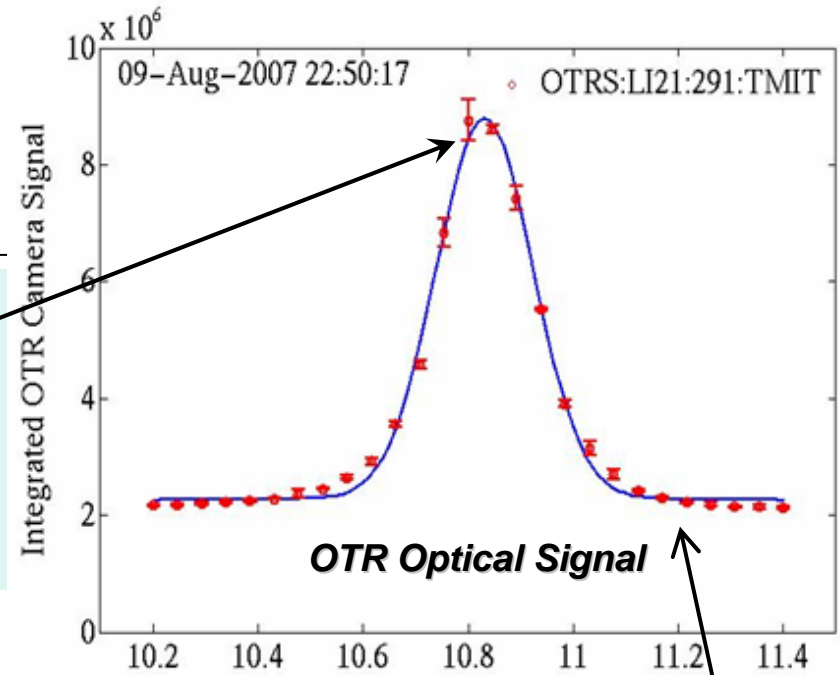
200 pC, extreme compression

Unexpected Physics! **Coherent OTR after 35-degree Bend, Even With No BC1**

Evidence for Micro-bunching:

QB*1.002

OTR signal peaks when quad is set for linear achromat, otherwise it damps micro-bunching

10 x 10^6
09-Aug-2007 22:50:17   ○ OTRS:LI21:291:TMIT

Integrated OTR Camera Signal

OTR Optical Signal

10.2   10.4   10.6   10.8   11   11.2   11.4

DL1 Quadrupole Strength

RF Gun
Gun Solenoid

Gun Spectrometer

L0a

L0b

RF Deflector

L1S

2-km point in 3-km SLAC linac ↑

X-band RF acc. section

BC1
OFF

L1S & L1X ON CREST

Cathode QE and Uniformity

18-AUG-2007 17:54:36, $QE = 3.68 \times 10^{-5}$, $R_{eff} = 0.338$ mm

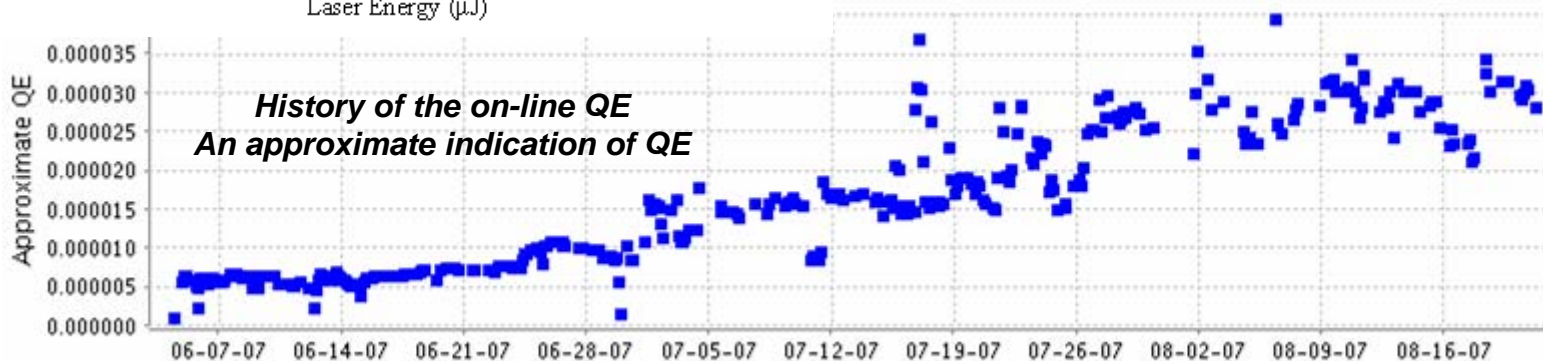*Emission Image of Cathode on YAG*
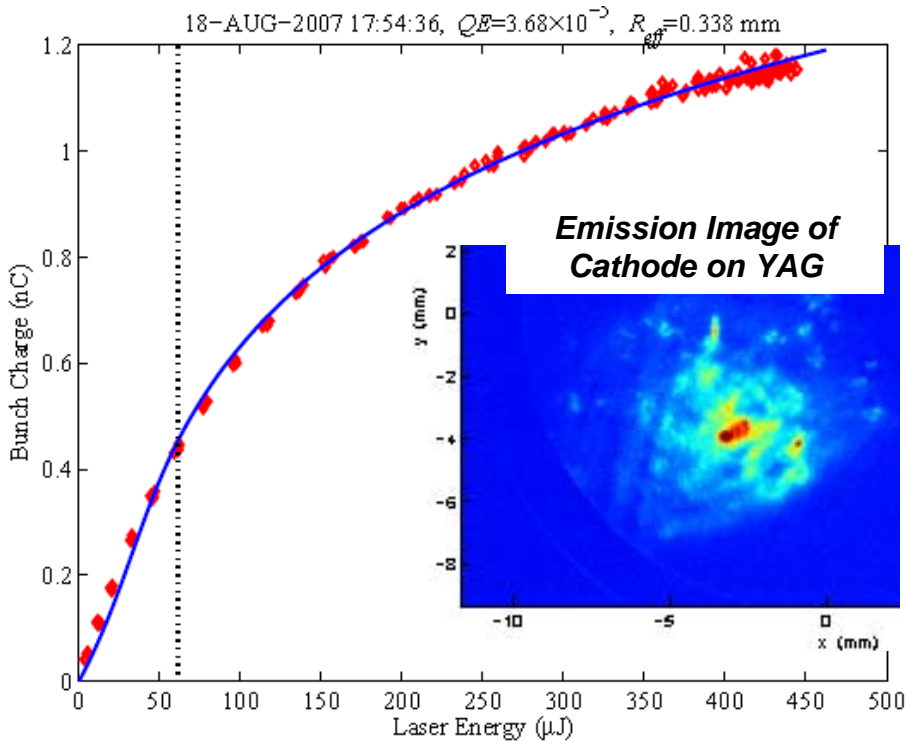
- **QE has been increasing due to constant exposure to the UV laser and by actively Laser Cleaning the cathode.**

- **QE is now ~3×10^{-5}, 2 times lower than spec (6×10^{-5}).**

- **QE-scans show emission is in the Space Charge Limited Regime at 1nC for a 1.3 mm dia. laser on the cathode.**

*History of the on-line QE
An approximate indication of QE*

Structured Cathodes Sensitive at Fundamental of TiS (~900nm)

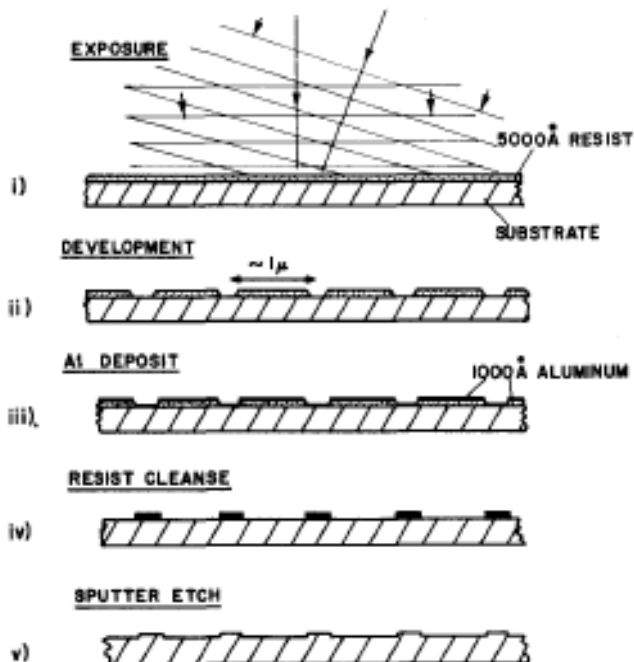## Fabrication of S1-cathode over a structured substrate

FIG. 2. Method for producing shallow-etched gratings. A split laser beam is used to expose striped areas of precise period in a resist. The resist is developed, aluminum coated, and cleaned off leaving Al stripes. An easily controlled 100—300-Å sputter etch is carried out, followed by removal of residual aluminum.
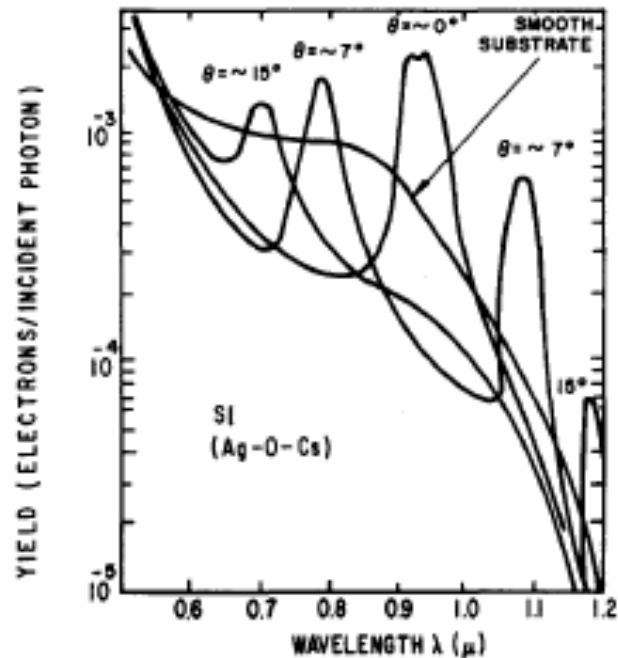

FIG. 3. Quantum efficiency of a grating-tuned S1 cathode. Shown are quantum efficiency curves vs free–space wavelength for *p*-polarized light at normal and at 7° and 15° angles of incidence. Response of a similar S1 on a smooth substrate is shown for comparison.

J.G. Endriz, Applied Physics Letters, 25,1974 p261

Need to study:
1. **Compatibility with copper or other metallic substrate**
2. **Vacuum requirements and long term stability: Approach for installation in gun**
3. **Thermal emittance: Theory and Expt.**
4. **Temporal response**